# Multiscaling of Galactic Cosmic Ray Flux

A. Bershadskii

[1]ICAR, P.O. Box 31155, Jerusalem 91000, Israel
and Kavli Institute for Theoretical Physics, University of California, Santa Barbara, California 93106-4030
(Received 7 July 2002; revised manuscript received 5 August 2002; published 31 January 2003)

Multiscaling analysis of the differential flux dissipation rate of galactic cosmic rays (carbon nuclei) is performed in the energy ranges 56.3–73.4 MeV/nucleon and 183.1–198.7 MeV/nucleon, using the data collected by the ACE/CRIS spacecraft instrument for the year 2000. The analysis reveals strong (turbulencelike) intermittency of the flux dissipation rate for short-term intervals: 1–30 h. It is also found that the type of intermittency can be different in different energy ranges.

DOI: 10.1103/PhysRevLett.90.041101 PACS numbers: 96.40.Kk, 52.30.Cv, 95.30.Qd

*Introduction.*—Galactic cosmic rays (GCR) originate outside the solar system. They comprise protons (85%), alpha particles (14%), and heavy nuclei. Interaction with a large-scale ordered magnetic field causes the gradient- and curvature-drift motion of GCR in the inner heliosphere, while the interaction with the irregular (stochastic) field component results in the pitch angle scattering of GCR. The scale sizes for the two effects, drifts which depend on variations in the mean field on the order of the heliocentric radial distance, and diffusion which depends on irregularities of sizes comparable to the particles gyroradii, are quite distinct (see, for instance [1,2], and references therein).

Until recently space instruments have lacked the combination of large geometrical factors and good mass resolution required to address the question of the variation on *short* time scales of individual nuclides other than H and He. In the present Letter we report on an investigation of the flux fluctuations of GCR nuclei (carbon, $Z = 6$) based on the Advanced Composition Explorer (ACE) spacecraft data. The intensities of these low-energy particles have been continuously monitored by the Cosmic Ray Isotope Spectrometer (CRIS).

In order to get away from the effects of the Earth's magnetic field, the ACE spacecraft orbits at the L1 libration point which is a point of Earth-Sun gravitational equilibrium about $1.5 \times 10^6$ km from Earth and $148.5 \times 10^6$ km from the Sun.

The large collecting power and high resolution of the CRIS instrument allows investigation of GCR flux dynamics on short time scales (beginning from 1 h) and in different energy ranges.

Current theories of parallel and perpendicular diffusion are fairly well accepted for high-energy particles. However, there are important outstanding issues pertaining to diffusion and transport of charged particles at medium to low energies [3].

Multiscaling properties of cosmic rays have been already discussed in the light of the data obtained by neutron monitors with cutoff rigidity 1.09 GeV (see, for instance, [4,5], and references therein) as well as modulation of the cosmic rays by solar wind turbulence and magnetic field intermittency [6–12]. However, as far as we know, multiscaling analysis of the GCR heavy nuclei data obtained by satellite instruments is performed here for the first time. This analysis reveals a strong (turbulent-like) intermittency of the GCR dissipation rate and dependence of the intermittency type on the energy range (not to be confused with the high-energy physics intermittency [13,14]). These empirical results are difficult to understand theoretically. It is possible that the observed multiscaling is a result of interstellar rather than interplanetary modulation (see Discussion). In any way, the relation between turbulence and cosmic ray transport is a challenging and exciting issue that deserves more attention.

*Dissipation rate of differential flux.*—Differential flux of the GCR, $J$, as measured by CRIS, is proportional to the normal component of the random cosmic ray speeds, $u$, and to their local concentration, $n$,

$$J \sim un. \tag{1}$$

Fluctuations of $J$ with time are then determined by corresponding fluctuations of $u$ and $n$.

Dissipation of passive admixture concentration in fluid turbulence is characterized by a "gradient" measure [15–17]:

$$\chi_r = \frac{\int_{v_r} (\nabla n)^2 dv}{v_r}, \tag{2}$$

where $v_r$ is a subvolume with space scale $r$ (for detailed justification of this measure, see the handbook [15], p. 381 and further). The scaling law of this measure moment,

$$\langle \chi_r^p \rangle \sim r^{-\mu_p}, \tag{3}$$

is an important characteristic of the dissipation rate field just in the *inertial* interval of turbulence (see, for instance, [15–17]). An analogous measure is used to characterize also the dissipation rate of turbulent velocity (or kinetic energy) in the inertial interval of scales [15–17].

  

For turbulent flows the Taylor hypothesis is generally used to interpret the data [6,12,16]. This hypothesis states that the intrinsic time dependence of the wave fields ($u$ and $n$) can be ignored when the turbulence is convected past the probes at nearly constant speed. With this hypothesis, the temporal dynamics should reflect the spatial one, i.e., the fluctuating velocity (concentration) field measured by a given probe as a function of time; $u(t)$ is the same as the velocity $u(x/\langle u\rangle)$, where $\langle u\rangle$ is the mean velocity and $x$ is the distance to a position "upstream" where the velocity is measured at $t = 0$.

With the Taylor hypothesis $dJ/dx$ is replaced by $dJ/\langle u\rangle dt$ and one can define GCR flux dissipation rate as

$$\chi_\tau \sim \frac{\int_0^\tau (\frac{dJ}{dt})^2 dt}{\tau}, \tag{4}$$

where $\tau \simeq r/\langle u\rangle$ and the corresponding scaling of the dissipation rate moments as [17]

$$\langle \chi_\tau^p \rangle \sim \tau^{-\mu_p}. \tag{5}$$

Substituting (1) into (4) one can estimate the GCR flux dissipation rate through characteristics of $u$ and $n$. We can consider two asymptotic regimes. For sufficiently small GCR energies the flux dissipation rate has been dominated by the concentration dissipation:

$$\langle \chi_\tau^p \rangle \sim \left\langle \left[ \frac{1}{\tau} \int_0^\tau \left( \frac{dn}{dt} \right)^2 dt \right]^p \right\rangle \sim \tau^{-\mu_p}, \tag{6}$$

while for sufficiently large GCR energies the flux dissipation rate has been dominated by the energy (velocity) dissipation:

$$\langle \chi_\tau^p \rangle \sim \left\langle \left[ \frac{1}{\tau} \int_0^\tau \left( \frac{du}{dt} \right)^2 dt \right]^p \right\rangle \sim \tau^{-\mu_p}. \tag{7}$$

Because the CRIS instrument measures the differential flux ($J$), but not the velocity $u$ and concentration $n$ separately, this interpretation can be considered as a qualitative one only (see Discussion). In particular, at this interpretation $u$ for the GCR is considered as the "markers" velocity for some continuous velocity field and $n$ is considered as the markers space concentration. In any way, we will calculate the dissipation $\chi_\tau$ using definition (4), where the GCR flux $J(t)$ will be taken directly from the CRIS data (see next section).

*The data.*—We will use the data collected by the ACE/CRIS instrument during the year 2000 (the year of maximum solar activity). We will consider carbon nuclei, C ($Z = 6$). Carbon is the lightest abundant nuclei (after H and He) in the ACE/CRIS collection. As we shall see this fact allows consideration of both asymptotes mentioned in the previous section.

Figure 1(a) shows scaling of the GCR flux dissipation rate moments $\langle \chi_\tau^p \rangle$ (4) and (5) for the C nuclei with energies from energy range 56.3–73.4 MeV/nucleon (the lowest energy range in the ACE/CRIS collection for carbon).

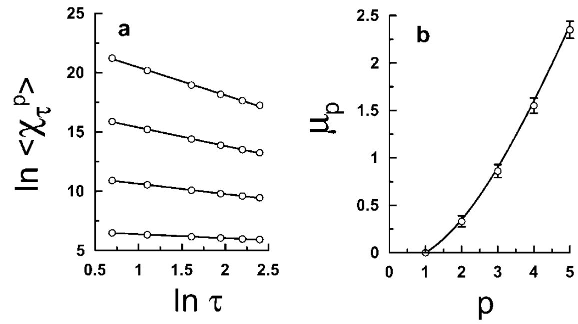


FIG. 1. (a) The GCR flux dissipation rate moments $\langle \chi_\tau^p \rangle$ against $\tau$ for the C nuclei with energies from the energy range 56.3–73.4 MeV/nucleon. The time interval $\tau$ is measured in hours, whereas the GCR differential flux $J$ is measured in $10^{-7.5}$ particles/m$^2$ s sr MeV. Log-log scales are chosen in the figure for comparison with scaling Eq. (5). The straight lines (the best fit) are drawn to indicate the scaling. The upper data sets correspond to larger $p = 2, 3, 4, 5$. (b) The scaling exponents $\mu_p$ (circles) extracted from (a). The solid curve corresponds to the intermittency exponents $\mu_p$ obtained for the inertial-convective region of a passive admixture concentration dissipation rate in a laboratory turbulent air flow [17].

Figure 1(b) shows the scaling exponents $\mu_p$ (circles) extracted from Fig. 1(a) [as slopes of the straight lines cf.(5)]. The solid curve in Fig. 1(b) corresponds to the intermittency exponents $\mu_p$ obtained for the inertial-convective region of a passive admixture concentration in a laboratory turbulent air flow [17]. To support the striking correspondence between the two data sets multiscaling let us calculate also the extended self-similarity (ESS [18]) exponents, $\beta_p$, extracted from the equation

$$\langle \chi_\tau^p \rangle \sim \langle \chi_\tau^3 \rangle^{\beta_p}. \tag{8}$$

The ESS of type (8) usually has clearer scaling form than ordinary scaling (5) and covers a wider range of scales (see [18] for a review of ESS and for examples). Figure 2(a) shows the ESS of the GCR flux dissipation rate moments $\langle \chi_\tau^p \rangle$ (8) using log-log scales. The straight lines (the best fit) are drawn to indicate the ESS (8). Figure 2(b) shows the ESS exponents $\beta_p$ (circles) extracted from Fig. 2(a) [as slopes of the straight lines cf.(8)]. The solid curve in Fig. 2(b) corresponds to the intermittency exponents $\beta_p$ obtained for the inertial-convective region of passive admixture concentration in different laboratory turbulent flows [17].

Now let us turn to the data corresponding to the energy range with the highest carbon nuclei energies observed by ACE/CRIS. Figure 3(a) shows scaling of the GCR flux dissipation rate moments $\langle \chi_\tau^p \rangle$ (4) and (5) for the C nuclei with energies from energy range 183.1–198.7 MeV/nucleon.

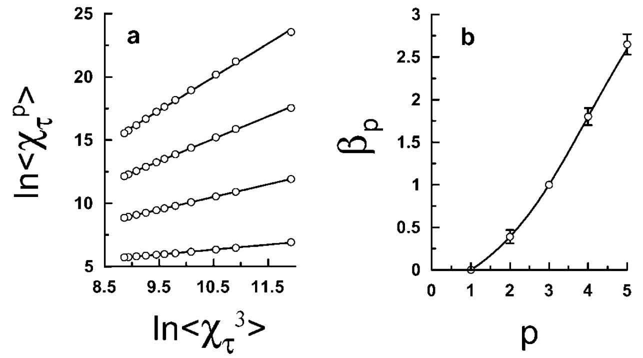


FIG. 2. (a) The ESS of the GCR flux dissipation rate moments $\langle\chi_\tau^p\rangle$ against $\langle\chi_\tau^3\rangle$ in log-log scales (8) for the energy range 56.3–73.4 MeV/nucleon. The straight lines (the best fit) are drawn to indicate the ESS (8). The upper data sets correspond to larger $p = 2, 3, 4, 5$. (b). The ESS exponents $\beta_p$ (circles) extracted from (a). The solid curve corresponds to the intermittency exponents $\beta_p$ obtained for the inertial-convective region of a passive admixture concentration dissipation rate in different fluid turbulent flows [17].

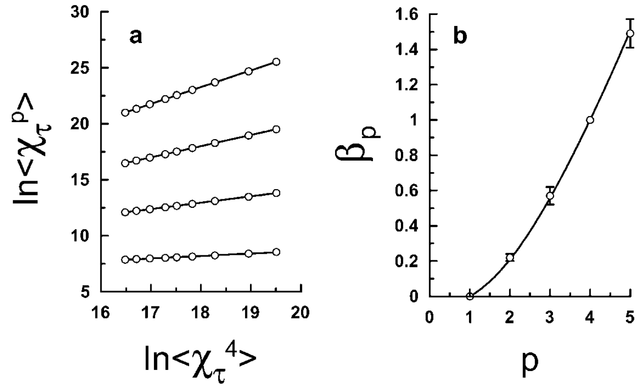


FIG. 4. (a) The ESS of the GCR flux dissipation rate moments $\langle\chi_\tau^p\rangle$ against $\langle\chi_\tau^3\rangle$ in log-log scales (9) for the energy range 183.1–198.7 MeV/nucleon. The straight lines (the best fit) are drawn to indicate the ESS (9). (b) The ESS exponents $\beta_p$ (circles) extracted from (a). The solid curve corresponds to the intermittency exponents $\beta_p$ calculated using the She-Leveque model.

Figure3(b) shows the scaling exponents $\mu_p$ (circles) extracted from 3(a) [as slopes of the straight lines cf. (5)]. The solid curve in Fig. 3(b) corresponds to the intermittency exponents $\mu_p$ calculated using the She-Leveque model [19], which is in very good agreement with the data for the *velocity* (kinetic energy dissipation) field intermittency obtained in the inertial interval for isotropic fluid turbulence. Figures 4(a) and 4(b) show corresponding ESS properties

$$\langle\chi_\tau^p\rangle \sim \langle\chi_\tau^4\rangle^{\beta_p} \tag{9}$$

observed for the data. Again, as in Fig. 3(b), correspondence to the fluid turbulence [energy dissipation rate, the solid curve in Fig. 4(b)] is very good.

The interval of time scales under consideration is 1–30 h. It seems to be useful to compare the observed properties of the GCR flux dissipation rate with relevant properties of the local interplanetary magnetic field. Figure 5 shows the energy spectrum of the 3D magnetic field magnitude measured by the ACE/MAG magnetometer in the same time intervals as the ACE/CRIS data. The slope $-5/3$ indicates Kolmogorov-like scaling (cf. [10]). Let us recall that the turbulent fluid dissipation rates used for comparison in Figs. 1–4 were obtained just for the inertial (inertial-convection) interval of scales where the Kolmogorov-like scaling should be expected [17,19].

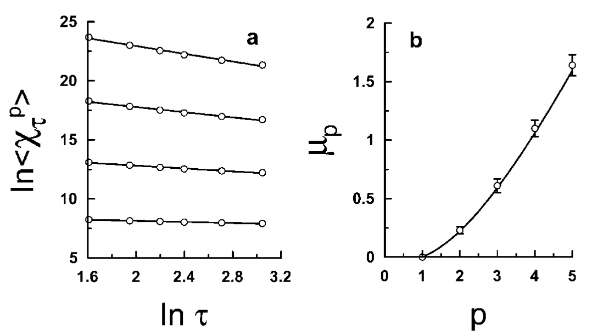


FIG. 3. (a) The GCR flux dissipation rate moments $\langle\chi_\tau^p\rangle$ (4) and (5) against $\tau$ for the C nuclei with energies from the energy range 183.1–198.7 MeV/nucleon. (b) The scaling exponents $\mu_p$ (circles) extracted from (a). The solid curve in (b) corresponds to the intermittency exponents $\mu_p$ calculated using the She-Leveque model for isotropic fluid turbulence [19].

*Discussion.*—The results in the previous section seem to be in agreement with the qualitative estimates made in the second section. For relatively small energies the flux dissipation rate behaves as one dominated by the GCR

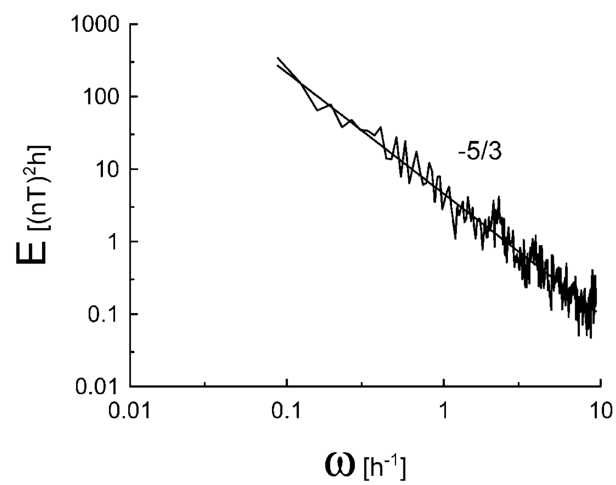


FIG. 5. Energy spectrum of 3D magnetic field magnitude measured by the ACE/MAG magnetometer in the discussed range of the time scales.

particle concentration dissipation rate, whereas for relatively large energies the GCR flux dissipation rate seems to be dominated by velocity (kinetic energy) dissipation.

Since the CRIS instrument measures the differential flux ($J$) only, but not the velocity of GCR ($u$) and the concentration ($n$) separately [cf. (1)], we have no idea about magnitudes of the fluctuations of $u$ and $n$ themselves. Therefore existence of the two asymptotes (6) and (7) is still a pure phenomenology (for the intermediate energies the scaling is deformed by competition between the two different mechanisms of the flux dissipation). The same reason (unknown $u$ and $n$ for the GCR) makes it impossible to perform any theoretical estimates for the scales of the GCR flux dissipation rate multiscaling.

Although correspondence between the motions in magnetohydrodynamics and hydrodynamic cases has been reported earlier (see, for instance, recently [20], and references therein), it is much more difficult to understand such detailed correspondence between cosmic rays and fluid turbulence, especially the physical means by which such energetic carbon ions become a passive component of the interplanetary turbulence (see below a brief discussion of another possibility related to *interstellar* turbulence). Indeed, as it follows from the previous two sections the observed GCR particle dissipation rate exhibits intermittent properties of a passive admixture convected by turbulent motion of a classic (isotropic, incompressible) nonmagnetic fluid. The solar wind [including the interplanetary magnetic field (IMF)] is certainly very different from such a fluid. Interaction of the electrically charged GCR particles with the solar wind and the magnetic field may be resonant (see, for instance, [7,8,20], and references therein). On the other hand, if the interplanetary plasma fluctuations are comprised of up to 80% quasi-two-dimensional fluctuations, as some believe [21,22], then that component would not resonantly scatter energetic carbon. In this case, however, we are dealing with a strong *anisotropy* that again leads us very far from isotropic fluid turbulence. Independent of that issue, the statistical result of the scattering is that the energetic cosmic rays follow the convection diffusion equation, and many components of the diffusion tensor are determined by the local turbulence properties of the solar wind. Even the fact that many characteristics of solar wind and IMF turbulence are known to be similar to those of the turbulence of classic nonmagnetic fluids (see [6–12], and references therein), the presumably resonancelike interactions of GCR particles with the solar wind and IMF or, alternatively, the strong anisotropy of the interplanetary plasma fluctuations seem to be nonconsistent with the picture observed here. These empirical results need reconsideration of our approach to stochastic *short*-term convection of the low-energy GCR particles (heavy nuclei) in the heliosphere and their *short*-term interactions with the solar wind and IMF. Moreover, from the present analysis we cannot give a compelling argument that it is just the interplanetary medium that is the origin of the turbulencelike multiscaling behavior of the carbon ions. The interstellar medium is also turbulent (see, for instance, [8,20]) and, at least the density spectrum, appears to be Kolmogorov. Might the multiscaling of carbon ions not be a consequence of their propagation through the interstellar medium, where the energy density of the cosmic rays as a whole is of the same order as that of the magnetic field? Such a turbulencelike multiscaling property might be quite natural in the interstellar medium rather than in the interplanetary one.

The author is grateful to the ACE/CRIS and the ACE/MAG instrument teams as well as to the ACE Science Center for providing the data. Numerous discussions on the subject with K. R. Sreenivasan were very useful for this investigation. This research was supported in part by the National Science Foundation under Grant No. PHY99-07949.

[1] L. A. Fisk and N. A. Schwadron, J. Geophys. Res. **100**, 7865 (1995).
[2] M.V. Alania, Acta Phys. Pol. B **33**, 1149 (2002).
[3] R. Schlickeiser, *Cosmic Ray Astrophysics* (Springer-Verlag, Berlin, 2002).
[4] K. Kudela and D. Venkatesan, Nucl. Phys. B, Proc. Suppl. **39**, 127 (1995).
[5] A. Bershadskii, J. Phys. G **27**, L61 (2001).
[6] T. S. Horbury, in *Plasma Turbulence and Energetic Particles*, edited by M. Ostrowski and R. Schlickeiser (Univ. Jagiellonian Press, Cracow, 1999), p. 28.
[7] B. Chandran, Phys. Rev. Lett. **85**, 4656 (2001).
[8] J. Cho, A. Lazarian, and E.T. Vishniac, astro-ph/0205286.
[9] O. Stawicki, S. P. Gary, and H. Li, J. Geophys. Res., Space Phys. **106**, 8273 (2001).
[10] M. L. Goldstein, Astrophys. Space Sci. **227**, 349 (2001).
[11] E. Marsch and S. Liu, Ann. Geophys. **11**, 227 (1993).
[12] T. S. Horbury and A. Balogh, Nonlinear Proc. Geophys. **4**, 185 (1997).
[13] A. Bialas and R. Peschanski, Nucl. Phys. **B273**, 703 (1986); **B308**, 857 (1988).
[14] A. Bershadskii, Phys. Rev. C **59**, 364 (1999).
[15] A. C. Monin and A. M. Yaglom, *Statistical Fluid Mechanics* (MIT Press, Cambridge, 1975), Vol. 2.
[16] K. R. Sreenivasan, Annu. Rev. Fluid Mech. **23**, 539 (1991).
[17] K. R. Sreenivasan and R. A. Antonia, Annu. Rev. Fluid Mech. **29**, 435 (1997).
[18] R. Benzi, L. Biferale, S. Ciliberto, M.V. Struglia, and R. Tripiccione, Physica (Amsterdam) **96D**, 162 (1996).
[19] Z.-S. She and E. Leveque, Phys. Rev. Lett. **72**, 336 (1994).
[20] J. Cho, A. Lazarian, and E. T. Vishniac, Astrophys. J. **564**, 291 (2002).
[21] W. H. Matthaeus, M. L. Goldstein, and D. A. Roberts, J. Geophys. Res. **95**, 20673 (1990).
[22] J.W. Bieber, W. Wanner, and W. H. Matthaeus, J. Geophys. Res. **101**, 2511 (1996).